

Reinforced High-Strength Concrete Beams in Flexure

by M. A. Rashid and M. A. Mansur

Flexural test results generated on 16 reinforced concrete beams to evaluate the implications of using high-strength concrete (HSC) are reported. Test parameters considered include concrete compressive strength, ratios of tensile and compressive reinforcements, and spacing of lateral ties. It is found that the current code provisions for serviceability requirements of maximum crack width and ultimate strength are adequate up to a concrete strength of approximately 130 MPa. Concerns, however, are expressed regarding the adequacy of those for cracking moment and service load deflection. It is shown that stresses generated by shrinkage of concrete and the creep associated with it can significantly affect the cracking moment and service load deflection of reinforced HSC beams. Also, some detailing requirements for compression reinforcement need to be reassessed so as to utilize its full strength potential and ensure adequate ductile response of the beam when HSC is involved.

Keywords: beam; crack; deflection; ductility; flexural strength; high-strength concrete; reinforced concrete.

INTRODUCTION

Despite a large number of investigations¹⁻¹⁵ carried out in the past on flexural behavior of high-strength concrete (HSC) beams, controversy still remains with regard to some vital design issues. One such issue is the serviceability requirement of deflection. Beams tested by several investigators consistently demonstrated significantly larger deflections at service load than what would be predicted by following the ACI Code¹⁶ provisions. Even the assumption of cracked moment of inertia as the effective value and use of the representative expressions for the elastic modulus of concrete as reported by ACI Committee 363¹⁷ for HSC had failed to bring the predictions on the conservative side. Therefore, explanations must be sought through further investigations.

Another important design issue is the ductility or the ability of a reinforced concrete (RC) member to deform at or near the ultimate load without significant strength loss. Because concrete becomes increasingly more brittle as its compressive strength is increased, guaranteeing adequate ductility represents one of the primary design concerns when HSC is involved. Based on the current code provisions, it can be analytically shown¹⁸ that, everything else remaining the same, an increase in concrete strength leads to higher ductility. Experimental evidence reported by many researchers^{2-6,9,10,12-14} supports this prediction, except for those by Ashour¹ and Shin, Ghosh, and Moreno.¹⁹ In these cases, test results have also shown enhanced ductility for higher strength concrete beams, but only up to a concrete strength of around 80 MPa. Thereafter, ductility decreases as the concrete strength is increased. Further experimental evidence, embracing concrete with compressive strength greater than 80 MPa, is therefore necessary with analytical backing.

In view of this, the present study aims at investigating the full flexural response of reinforced HSC beams with concrete compressive strengths ranging from 40 to 130 MPa.

Particular emphasis has been given to the issues of deflection at service load and ductility. Relevant information has been collected from the literature whenever deemed necessary for the analysis and interpretation of test observations. Design provisions contained in the current codes of practices, particularly those in the ACI Code,¹⁶ have also been examined.

RESEARCH SIGNIFICANCE

The results of an investigation carried out on flexural behavior of reinforced HSC beams with a wide range of concrete strengths are presented in this paper. It presents useful information regarding the effects of shrinkage of concrete and the resulting creep on cracking moment and service load deflection and the effect of concrete strength on ductility. It has been shown that the upper limit of tensile reinforcement ratio needs to be reduced and that some detailing requirements regarding the ties are necessary to ensure adequate ductile response for HSC beams. The controversial issues discussed herein for evaluating the performance of HSC beams would be beneficial to researchers and structural designers.

EXPERIMENTAL PROGRAM

Test specimens and material properties

The program consisted of testing 16 beams with concrete strength f'_c ratios of tensile and compressive reinforcement (ρ and ρ' , respectively) and spacing s of lateral ties as the main parameters. The details of test beams are presented in Table 1 and Fig. 1, where one letter followed by three numerals, such as A111 or B312, designate the specimens. The letters A, B, C, D, and E stand for f'_c of 42.8, 72.8 to 77.0, 85.6 to 88.1, 114.5, and 126.2 MPa, respectively. The first numeral—1, 2, 3, 4, or 5—indicates the tensile reinforcement ratio in percentage, rounded off to the previous whole number. The second numeral—1, 2, or 3—indicates the minimum, twice the minimum, and thrice the minimum ratio of compression reinforcement, respectively, while the third numeral—1, 2, or 3—stands for the similar quantities of the volumetric ratio of lateral ties ρ_s (as defined in the section entitled “Ductility”). Beam B211a was identical to Beam B211 as complete information for the latter could not be captured due to malfunctioning of the computer at 93% of its maximum load capacity.

Figure 1 shows reinforcement details of test beams. When more than one layer of bars was needed (maximum of four bars in a single layer), a clear spacing of 25 mm was maintained between the layers, and larger-diameter bars were placed at the bottom layer when different sizes of bars were

ACI Structural Journal, V. 102, No. 3, May-June 2005.

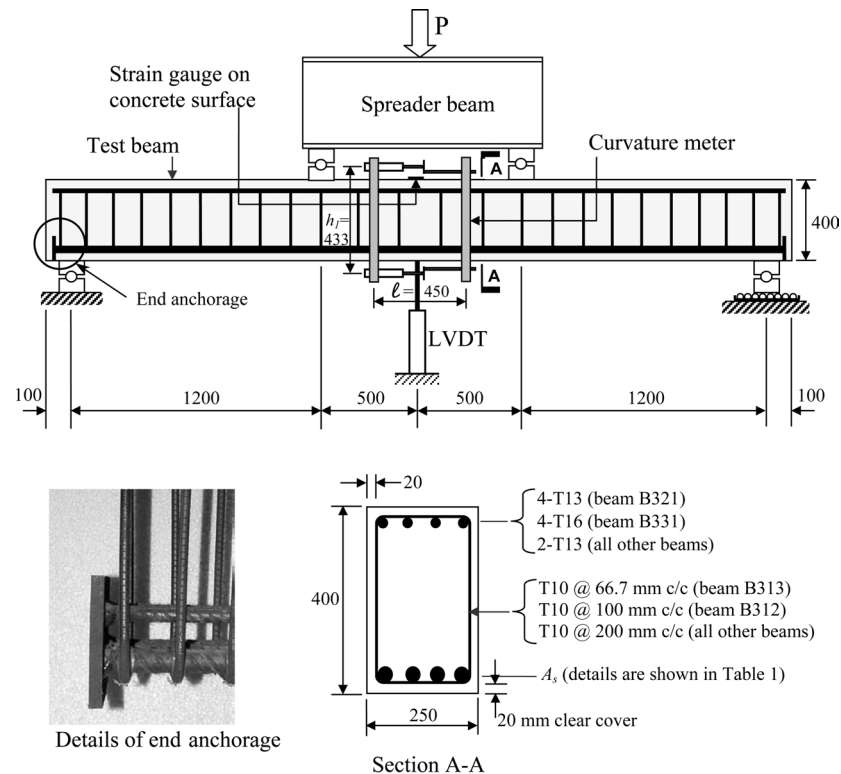
MS No. 04-072 received January 29, 2004, and reviewed under Institute publication policies. Copyright © 2005, American Concrete Institute. All rights reserved, including the making of copies unless permission is obtained from the copyright proprietors. Pertinent discussion including author's closure, if any, will be published in the March-April 2006 ACI Structural Journal if the discussion is received by November 1, 2005.

M. A. Rashid is an associate professor in the Department of Civil Engineering and Director of Planning and Development at Dhaka University of Engineering & Technology, Gazipur, Bangladesh.

M. A. Mansur is a visiting scholar in the Department of Civil and Environmental Engineering at the University of Michigan, Ann Arbor, Mich.

involved. For anchorage, a steel plate was welded at each end of all tensile bars, as can be seen in Fig. 1.

The yield strengths f_y of longitudinal steel bars used were 460, 537, 466, and 472 MPa for T25, T20, T16, and T13 bars, respectively (T denotes high-yield deformed bars, and



(Note: all dimensions are in mm)

Fig. 1—Experimental setup and details of test beams.

Table 1—Details of test beams and summary of test results

Beam	Concrete strength $f'_{c,100}$, [*] MPa	Longitudinal tensile bars	Reinforcement ratio			Test results								Concrete strain capacity, ϵ_{cu} [§]	Age of concrete days
			Tensile $\rho = A_s/bd$, %	Compression $\rho' = A'_s/bd$, %	Tie ρ_s , [†] %	Cracking load P_{cr} , kN	At yielding		At ultimate		At failure [‡]				
							Load P_y , kN	Deflection δ_y , mm	Load P_u , kN	Deflection δ_u , mm	Load P_f , kN	Deflection δ_f , mm			
A111	42.8	1-T25 + 2-T20	1.25	0.30	0.62	35.5	300.78	7.7	342.84	23.0	291.52	51.2	0.0035	39	
A211	42.8	4-T25	2.20	0.30	0.62	28.0	440.48	15.5	461.30	37.0	392.30	76.4	0.0033	42	
B211	74.6	4-T25	2.20	0.30	0.62	51.5	420.40	14.6	495.18	50.0	—	—	0.0038	42	
B211a	73.6	4-T25	2.20	0.30	0.62	64.0	456.70	14.9	500.90	42.0	426.62	91.6	0.0034	17	
B311	72.8	6-T25	3.46	0.31	0.62	49.0	575.68	17.0	751.96	26.1	639.76	28.3	0.0036	44	
B312	72.8	6-T25	3.46	0.31	1.23	40.0	560.36	16.9	730.22	24.4	619.86	49.9	0.0033	55	
B313	72.8	6-T25	3.46	0.31	1.85	42.0	580.26	16.1	742.94	27.0	631.45	69.5	0.0037	57	
B321	77.0	6-T25	3.46	0.62	0.62	45.0	551.16	15.5	765.06	34.4	649.70	46.8	0.0036	50	
B331	72.8	6-T25	3.46	0.94	0.62	50.0	590.38	16.5	772.80	27.0	657.68	46.0	0.0033	51	
B411	77.0	8-T25	4.73	0.32	0.62	36.5	621.34	15.5	950.40	30.6	807.80	37.6	0.0039	52	
C211	85.6	4-T25 + 2-T16	2.71	0.30	0.62	52.0	560.94	18.2	650.42	44.1	552.20	58.1	0.0042	40	
C311	88.1	4-T25 + 4-T16	3.22	0.31	0.62	53.0	605.46	18.0	730.12	28.3	619.88	50.5	0.0030	64	
C411	85.6	6-T25 + 2-T20	4.26	0.32	0.62	45.0	722.56	19.3	901.40	29.0	769.60	36.1	0.0034	42	
C511	88.1	8-T25 + 2-T16	5.31	0.33	0.62	44.5	811.82	20.8	880.60	23.3	749.96	33.3	0.0027	67	
D211	114.5	4-T25	2.20	0.30	0.62	71.0	506.00	16.0	605.00	38.0	515.00	80.2	0.0032	28	
E211	126.2	4-T25	2.20	0.30	0.62	72.0	506.00	15.9	595.20	40.0	505.90	78.0	0.0030	45	

*Concrete compressive strength obtained from testing 100 x 200 mm cylinder.

†As obtained using Eq. (8).

‡Level corresponding to 85% of maximum load capacity in descending branch of load-deflection curve.

§Concrete compressive strain at initiation of concrete crushing.

||During testing, computer malfunctioned at load level of $0.93P_u$ in descending branch.

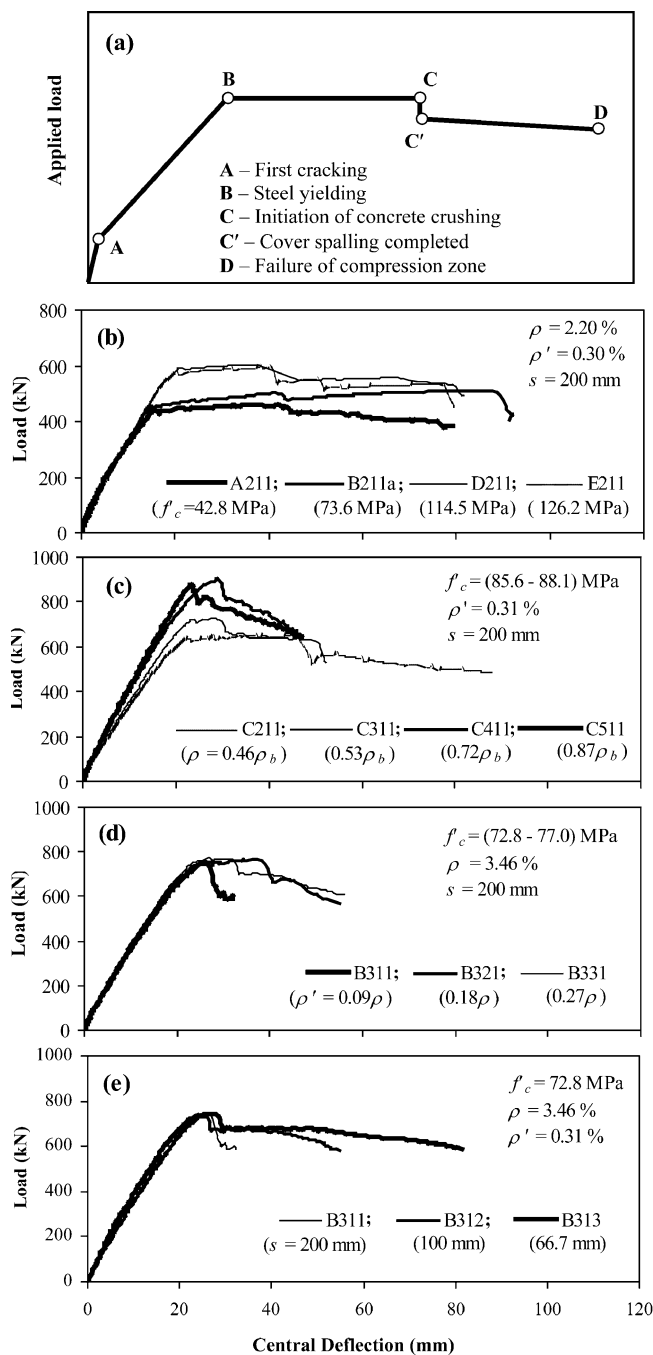


Fig. 2—Load versus central deflection response: (a) idealized curve; (b) concrete strength; (c) tensile reinforcement; (d) compression reinforcement; and (e) lateral closed ties.

the number following T indicates the diameter in mm). Ties were made up of T10 bars obtained from two different batches with yield strengths of 479 MPa for Beams B211, B211a, B311, B312, B321, B411, D211, and E211, and 541 MPa for the remaining beams.

Ready-mixed concrete was used for the beams in Series A, B (except B211a), and C, and those for Beams D211, E211, and B211a were prepared in the laboratory to achieve the target strength. The maximum size of coarse aggregates used was 10 mm. A sufficient number of 100 x 200 mm cylinders and 100 x 100 x 400 mm prisms were cast from each concrete mixture to determine the properties of concrete used.

Preparation and testing of specimens

All beams were cast in plywood molds. The beams and the control specimens were demolded the next day, cured for 14 days in a moist environment by using damp hessian, and then air-dried in the laboratory prior to testing.

The beams were tested under a four-point loading system over a span of 3400 mm (Fig. 1). The beams were suitably instrumented for measuring deflections at several locations including the midspan, curvature of the beam over a central gauge length of 450 mm, and concrete and steel strains at critical locations. Surface crack widths at the centerline of the bottom layer of tensile steel were measured within the central 600 mm length. The load was applied by a 2000 kN deflection-controlled hydraulic actuator. All strain and deformation readings were captured by a computer at preset load intervals until final collapse.

TEST RESULTS AND DISCUSSIONS

General behavior of beams

The experimental load-deflection curves, grouped according to the parameters considered, are presented in Fig. 2. It may be seen that four distinctly different segments, separated by four significant events that took place during the loading history, can idealize a typical load-deflection curve. Labeled as A, B, C, and D in Fig. 2(a), these events were identified as first cracking, yielding of tensile reinforcement, crushing with associated spalling of the concrete cover in the compression zone, and final disintegration of the compressed concrete as a consequence of either buckling of compression bars or fracture of the lateral ties or both, respectively. The first two events were associated with a reduction in beam stiffness, while the remaining two events led to a reduction in the applied load. In between two events, a straight line may approximate the curve.

The effects of different parameters on the load-deflection behavior of test beams are presented in Fig. 2(b) through (e). All beams behaved in a manner similar to the aforementioned description with the exception of those that contained either a higher amount of tensile reinforcement or a smaller amount of compression steel combined with a wider spacing of lateral ties. It can be clearly seen in Fig. 2(c) to (e) that, in these beams, the second and third events took place almost simultaneously, leading to a rapid loss in the load-carrying capacity. As all test beams were under-reinforced, yielding of tensile reinforcement was initiated before crushing of the cover concrete. Final failure, however, occurred due to disintegration of the confined concrete.

Cracking moment

In Table 2, the experimental cracking moments $M_{cr,exp}$ are compared with the corresponding moments calculated by using different approaches for the beams tested in this program. The first approach follows the ACI Code¹⁶ recommendations. Designated as $M_{cr,ACI}$, these moments are calculated using the following equation

$$M_{cr} = \frac{f_r I_g}{y_t} \quad (1)$$

where f_r is the modulus of rupture of concrete; I_g is the moment of inertia of the gross concrete section; and y_t is the distance of the extreme tension fiber from the neutral axis. It may be seen in Table 2 that the ACI Code¹⁶ procedure gives

Table 2—Predictions of cracking moment for high-strength concrete beams

Researcher(s)	No. of beams	Range of parameters considered			Ratio							
		Concrete strength f'_c , MPa	Tensile reinforcement ratio ρ , %	Compressive reinforcement ratio ρ' , %	$\frac{M_{cr,exp}}{M_{cr,ACI}}$		$\frac{M_{cr,exp}}{M_{cr,cal-1}}$		$\frac{M_{cr,exp}}{M_{cr,cal-2}}$		$\frac{M_{cr,exp}}{M_{cr,cal-3}}$	
					Mean	Standard deviation	Mean	Standard deviation	Mean	Standard deviation	Mean	Standard deviation
Present study	16	43 to 126	1.25 to 5.31	0.31 and 0.94	0.90	0.126	0.62	0.083	1.19	0.158	0.97	0.059
Ashour ¹	9	49 to 102	1.18 to 2.37	N/A*	1.02	0.131	0.69	0.124	0.85	0.162	0.82	0.148
Lambotte and Taerwe ⁶	6	34 to 81	0.48 to 1.45	N/A*	0.77	0.207	0.57	0.192	0.76	0.332	0.72	0.290
Paulson, Nilson, and Hover ⁷	9	37 to 91	1.49	0.0 to 1.49	0.68	0.114	0.49	0.118	0.80	0.393	0.74	0.317
Shin ¹⁰	28 [†]	27 to 100	0.41 to 3.60	0.41 to 3.60	1.00	0.216	0.71	0.190	0.93	0.393	0.89	0.339

*N/A = not available.

[†]Four out of a total of 32 beams have been excluded from consideration as, for those beams, predicted values of shrinkage stresses were found to be larger than those of corresponding modulus of rupture.

good predictions. It was shown, however, by Rashid, Mansur, and Paramasivam²⁰ that the ACI expression for f_r is highly conservative for HSC.

If a representative expression for modulus of rupture $f_r = 0.42(f'_c/150)^{0.68}$ as suggested by Rashid, Mansur, and Paramasivam,²⁰ is used in Eq. (1) to predict the cracking moment $M_{cr,cal-1}$, the beams display early cracking as depicted by a mean value of only 0.62 for the ratio $M_{cr,exp}/M_{cr,cal-1}$ with a standard deviation (SD) of 0.083 (Table 2). The key reason for early cracking of test beams may be attributed to the shrinkage^{21,22} of concrete with associated restraint provided by the embedded reinforcement. To account for this effect on cracking moment M_{cr} , a reduced tensile strength of concrete equal to $(f_r - f_{sh})$, where f_{sh} is the shrinkage-induced tension at the extreme fiber, is considered next. In this analysis, the free shrinkage strains ϵ_{sh} are calculated by following the procedure suggested by Gilbert.²³ This strain is then translated into the corresponding stress f_{sh} using the equivalent tensile force method as suggested by Large and Chen.²⁴ The values of the modulus of elasticity are estimated using the expression $E_c = 8900(f'_c/150)^{0.33}$ as suggested by Rashid, Mansur, and Paramasivam²⁰ for normal-strength concrete (NSC) as well as HSC. The cracking moments $M_{cr,cal-2}$, thus calculated, show a dramatic improvement in the predictions (Table 2), giving the mean value for the ratio $M_{cr,exp}/M_{cr,cal-2}$ of 1.19 and standard deviation of 0.158.

Realizing the fact that pretension induced by shrinkage is sustained in nature, an attempt has been made to include the effects of resulting creep to see if the predictions could be improved further. Inclusion of creep effects, however, complicates the analysis. In a situation like the present one, use of the usual creep factors for mature concrete under constant compressive stress is rather dubious because stresses in concrete due to shrinkage are built up gradually at a decreasing rate with time and are tensile in nature. Also, E_c of interest herein should refer to concrete in tension; it develops progressively from zero at the plastic state to its full value at the age under consideration.

The effective modulus method uses an aging coefficient $\chi(t, \tau_0)$ to obtain an age-adjusted effective modulus $\bar{E}_e(t, \tau_0)$, as given by

$$\bar{E}_e(t, \tau_0) = \frac{E_c(\tau_0)}{1 + \chi(t, \tau_0)\phi(t, \tau_0)} \quad (2)$$

where $E_c(\tau_0)$ is the modulus of elasticity of concrete at first loading, and $\phi(t, \tau_0)$ is the creep coefficient at time t for concrete first loaded at time τ_0 . An approximate value $\chi(t, \tau_0) = 0.80$ is frequently used for long-term creep analysis.^{21,25} As time approaches infinity, the creep coefficient is assumed to approach a final value, which usually falls within a range²³ between 1.5 and 4.0. Hence, for long-term creep analysis, the average value of the term $\chi(t, \tau_0)\phi(t, \tau_0)$ is usually taken as 2.2.

Because the nature of shrinkage-induced stress is different from that due to external loading, the usual values for coefficients $\chi(t, \tau_0)$ and $\phi(t, \tau_0)$ may not appropriately represent the resulting creep effects. While discussing the equivalent tensile force method for shrinkage curvature analysis, however, it was shown²⁶ that use of a reduced modulus \bar{E}_c equal to $E_c/2$, together with gross section properties, could account for the associated creep effect fairly accurately. This is equivalent to saying that the term $\chi(t, \tau_0)\phi(t, \tau_0)$ in Eq. (2) is equal to unity instead of an average value of 2.2 for long-term creep analysis for external loading. In the present attempt of evaluating the influence of shrinkage-induced creep effect on M_{cr} , it is assumed that the same approximation applies and that the modulus of elasticity in tension remains the same as that in compression, that is

$$\bar{E}_c = \frac{E_c}{2} \quad (3)$$

Cracking moments $M_{cr,cal-3}$, calculated by using this reduced modulus of elasticity along with f_{sh} , are compared with test results in Table 2. It may be seen that consideration of the shrinkage-induced creep effect gives closer predictions with the mean and SD for the ratio $M_{cr,exp}/M_{cr,cal-3}$ of 0.97 and 0.059, respectively. Similar calculations for the test data available in the literature^{1,6,7,10} also show further improvement in the prediction (Table 2) in terms of standard deviation. Inclusion of the resulting creep effect, however, slightly reduces the ratio. This is probably due to the fact that short-term creep marginally reduces the tensile stress induced by shrinkage, resulting in a slight increase in the calculated cracking-moment capacity.

From the preceding discussion, it appears that the use of a conservative expression for f_r , as suggested by the ACI Code,¹⁶ indirectly accounts for shrinkage and the associated creep effects in predicting the cracking moments.

Table 3—Predictions of maximum deflection at service load level for high-strength concrete beams

Researcher(s)	No. of beams	Range of parameters considered			Ratio							
		Concrete strength f'_c , MPa	Tensile reinforcement ratio ρ , %	Compressive reinforcement ratio ρ' , %	$\frac{\delta_{s,exp}}{\delta_{s,ACI}}$		$\frac{\delta_{s,exp}}{\delta_{s,cal-1}}$		$\frac{\delta_{s,exp}}{\delta_{s,cal-2}}$		$\frac{\delta_{s,exp}}{\delta_{s,cal-3}}$	
					Mean	Standard deviation	Mean	Standard deviation	Mean	Standard deviation	Mean*	Standard deviation*
Present study	16	43 to 126	1.25 to 5.31	0.31 to 0.94	1.26	0.082	1.23	0.066	1.22	0.068	0.93	0.059
Ashour ¹	9	49 to 102	1.18 to 2.37	—	1.17	0.065	1.23	0.161	1.18	0.094	0.91	0.053
Lin, Ling, and Hwang ⁵	9	27 to 69	2.04 to 3.67	0.34	1.27	0.121	1.27	0.109	1.26	0.110	0.96	0.089
Lambotte and Taerwe ⁶	5 [†]	34 to 81	0.48 to 1.45	—	1.17	0.116	1.33	0.313	1.21	0.183	0.94	0.082
Paulson, Nilson, and Hover ⁷	9	37 to 91	1.49	0.0 to 1.49	1.37	0.141	1.68	0.351	1.38	0.176	1.06	0.080
Shin ¹⁰	23 [‡]	27 to 100	0.41 to 3.60	0.41 to 3.60	1.56	0.272	2.03	0.761	1.75	0.501	1.26	0.243
Pastor, Nilson, and Slate ¹²	12	26 to 64	1.12 to 5.33	0.0 to 2.50	1.09	0.078	1.10	0.080	1.08	0.077	0.84	0.083

*For all of 67 literature^{1,5-7,10,12} beams considered, mean and standard deviation of ratio $\delta_{s,exp}/\delta_{s,cal-3}$ are 1.04 and 0.226, respectively.

[†]One out of total of six beams has been excluded from consideration as, for that beam, ratio of maximum moment to cracking moment ratio (M_d/M_{cr}) was close to unity.

[‡]Eight out of a total of 31 beams have been excluded from consideration for same reason as mentioned in preceding note.

Maximum deflection at service load

To investigate the service load behavior with respect to deflection, maximum (midspan) deflections $\delta_{s,cal}$ at service load (experimental ultimate load $P_{u,exp}$ divided by a factor of 1.7) are calculated for the test beams using the elastic bending theory as

$$\delta_{s,cal} = \frac{M_a}{24E_c I} (3L^2 - 4a^2) \quad (4)$$

in which M_a is the applied maximum (midspan) moment; L is the beam span; a is the shear span; E_c is the modulus of elasticity of concrete; and the moment of inertia I is taken as that specified by the ACI Code¹⁶ for effective moment of inertia I_e as

$$I_e = I_{cr} + (I_g - I_{cr}) \left(\frac{M_{cr}}{M_a} \right)^3 \leq I_g \quad (5)$$

in which I_g and I_{cr} are the moments of inertia of gross and cracked sections, respectively.

Comparisons between the calculated and the corresponding experimental deflections at service load, as shown in Table 3, indicate that the use of ACI Code¹⁶ expressions for f_r and E_c leads to highly unconservative predictions ($\delta_{s,ACI}$). Use of $f_r = 0.42(f'_{c,150})^{0.68}$ and $E_c = 8900(f'_{c,150})^{0.33}$, as suggested by Rashid, Mansur, and Paramasivam,²⁰ also yields no improvement in the predictions $\delta_{s,cal-1}$ as the mean and SD of the ratio $\delta_{s,exp}/\delta_{s,cal-1}$ are 1.23 and 0.066, respectively. Similar observations have also been reported by Pastor, Nilson, and Slate¹² and Paulson, Nilson, and Hover⁷ for reinforced HSC beams. Pastor, Nilson, and Slate¹² reported that even the assumption of a fully cracked beam, that is, use of $I_e = I_{cr}$, was of little benefit. Analysis of a large number of relevant test data on HSC beams, collected from the literature,^{1,5-7,10,12} provides further evidence (Table 3) that this method gives an unconservative estimate for service load deflection of HSC beams. The underlying reason should then

lie on shrinkage of concrete and the resulting creep effect, which modify both E_c and M_{cr} required in the analysis.

To explore this possibility, two sets of calculations have been performed: one by considering shrinkage-induced stresses alone and the other by including the associated creep effects as well, similar to what has been done for cracking moments ($M_{cr,cal-2}$ and $M_{cr,cal-3}$, respectively). Representative expressions for f_r and E_c , as suggested by Rashid, Mansur, and Paramasivam,²⁰ have been considered for both of the cases. For the second set, it is further assumed that the same reduction for E_c applies to concrete both in tension and compression, and that the subsequent deformation due to short-term applied loading is related to this reduced modulus. The service-load deflections calculated accordingly are denoted by $\delta_{s,cal-2}$ and $\delta_{s,cal-3}$, respectively. These values are compared with the respective experimental data and are presented in Table 3.

It may be seen in Table 3 that consideration of shrinkage-induced stresses alone gives less than 1% improvement for the test beams. If the associated creep effect is included, however, predictions improve dramatically. For the test beams, the mean and SD of the ratio $\delta_{s,exp}/\delta_{s,cal-3}$ are 0.93 and 0.059, respectively. Similar observations can also be made for 67 beams considered herein from the literature^{1,5-7,10,12} for which the ratio $\delta_{s,exp}/\delta_{s,cal-3}$ has a mean value of 1.04 and an SD of 0.226.

Maximum crack width at service load

The maximum crack widths $\omega_{cr,exp}$ measured at the center of the bottom layer of tensile reinforcement at the assumed service load are presented in Table 4. It may be seen from the results of Beams C211, C311, C411, and C511 that the effect of the amount of tensile reinforcement on the maximum crack width is relatively insignificant compared with that of concrete strength. Test results of Beams A211, B211, D211, and E211 indicate that the maximum crack width at the service-load level increases as the concrete strength is increased.

For analytical evaluation, expressions suggested by Gergely and Lutz²⁷ and those recommended in BS8110²⁸ have been chosen for assessment. In Table 4, the experimental maximum crack widths are compared with the corresponding predicted values, denoted as $\omega_{cr,G\&L}$ and $\omega_{cr,BS}$,

Table 4—Predictions of maximum crack width for test beams at service loads

Beam	Maximum crack width $\omega_{cr,exp}$, mm	Ratio	
		$\frac{\omega_{cr,exp}}{\omega_{cr,G\&L}}$	$\frac{\omega_{cr,exp}}{\omega_{cr,BS}}$
A111	0.22	0.93	1.65
A211	0.17	1.07	1.52
B211	0.19	1.11	1.57
B211a	0.18	1.04	1.47
B311	0.18	0.90	1.21
B312	0.19	1.02	1.36
B313	0.15	0.77	1.03
B321	0.18	0.91	1.21
B331	0.18	0.92	1.23
B411	0.34	1.79	2.23
C211	0.24	1.23	1.70
C311	0.24	1.24	1.67
C411	0.23	1.19	1.51
C511	0.22	1.31	1.63
D211	0.24	1.15	1.62
E211	0.22	1.09	1.54
Mean		1.10 (1.06)*	1.51 (1.46)*
Standard deviation		0.236 (0.152)*	0.276 (0.205)*

*Excluding that for Beam B411.

respectively. It may be noted that BS8110²⁸ specifications highly underestimate the crack widths for the test beams. The expression suggested by Gergely and Lutz,²⁷ however, gives good predictions (although it is unconservative for several beams). Excluding the result of Beam B411, which demonstrated a large crack width for an unknown reason, the mean and SD of the ratio $\omega_{cr,exp}/\omega_{cr,G\&L}$ are found to be 1.06 and 0.152, respectively.

Ultimate strength

The experimental ultimate strength corresponding to the initiation of concrete crushing, expressed as moment $M_{u,exp}$, is compared with that predicted by the ACI Code¹⁶ $M_{u,ACI}$ as shown in Table 5. It may be seen that the ACI Code¹⁶ provisions give a reasonable conservative estimate for the ultimate moment capacity of the test beams with a mean of 1.09 and SD of 0.072 for the ratio of experimental-to-predicted values.

To furnish additional evidence in support of the ACI Code¹⁶ provisions, the experimental ultimate moments of a large number of HSC beams, collected from the literature,^{1,3,5,6,10,12,15} are compared with the respective calculated values in Table 5. Once again, good agreement is found between the measured and the estimated values. For a total of 93 beams, the ratio $M_{u,exp}/M_{u,ACI}$ has an average value of 1.12 and an SD of 0.120.

Ductility

Ductility of a structural member may be defined as its ability to deform at or near the failure load without a significant loss in strength. In the case of a flexural member, sectional ductility based on curvature and/or member ductility based on deflection is usually considered. In the present study, attempts were made to continuously monitor the curvature within the central pure bending zone and deflection at midspan of the

Table 5—Predictions of ultimate moment for high-strength concrete beams

Researcher(s)	No. of beams studied	Range of f'_c considered, MPa	Ratio, $\frac{M_{u,exp}}{M_{u,ACI}}$	
			Mean*	Standard deviation*
Present study	16	43 to 126	1.09	0.072
Ashour ¹	9	49 to 102	1.02	0.032
Sarker, Adwan, and Munday ³	13	65 to 91	1.07	0.097
Lin, Ling, and Hwang ⁵	9	27 to 69	1.09	0.117
Lambotte and Taerwe ⁶	6	34 to 81	1.00	0.043
Shin ¹⁰	32	27 to 100	1.19	0.111
Pastor, Nilson, and Slate ¹²	12	26 to 64	1.09	0.067
Leslie, Rajagopalan, and Everard ¹⁵	12	64 to 81	1.16	0.146

*For all 93 literature^{1,3,5,6,10,12,15} beams considered, mean and standard deviation of ratio $M_{u,exp}/M_{u,ACI}$ are 1.12 and 0.120, respectively.

beams. Unfortunately, information acquired on curvature was incomplete because the curvature meter used lost its contact as soon as the unconfined concrete cover spalled off. The following discussion on the influence of various test parameters is therefore based on deflection ductility index μ_d , defined as

$$\mu_d = \frac{\delta_f}{\delta_y} \quad (6)$$

in which δ_f and δ_y are the maximum (midspan) deflections of the beam at failure and at yielding of the longitudinal tensile reinforcement, respectively. Herein, failure is assumed to have occurred at a load equal to 85% of the maximum load in the descending branch of the load-deflection curve.

Influence of concrete strength on ductility—Figure 3(a) shows a plot of ductility index μ_d as a function of concrete strength for the beams tested in this program. It may be seen that μ_d increases with an increase in concrete strength, but up to certain level of f'_c . Beyond this level, ductility decreases as the concrete strength is increased. Several researchers^{1,19} dealing with HSC beams reported similar observations for both singly and doubly reinforced beams.

To investigate whether or not the aforementioned trend can be confirmed analytically, a fictitious beam having the same dimensions and reinforcement details as beam A211 is considered for analysis. Instead of μ_d that is more difficult to calculate accurately, however, assessment has been made on curvature ductility μ_c , defined as the ratio of curvature at failure to that at yield. Herein, the beam is assumed to have failed when the extreme compression fiber of the confined concrete core reaches a strain capacity ϵ_{max} , suggested by Scott, Park, and Priestley²⁹ as

$$\epsilon_{max} = 0.004 + 0.9\rho_s \left[\frac{f_y''}{300} \right] \quad (7)$$

in which ρ_s and f_y'' are the volumetric ratio and yield strength, respectively, of lateral tie bars. The values of ρ_s have been obtained as follows

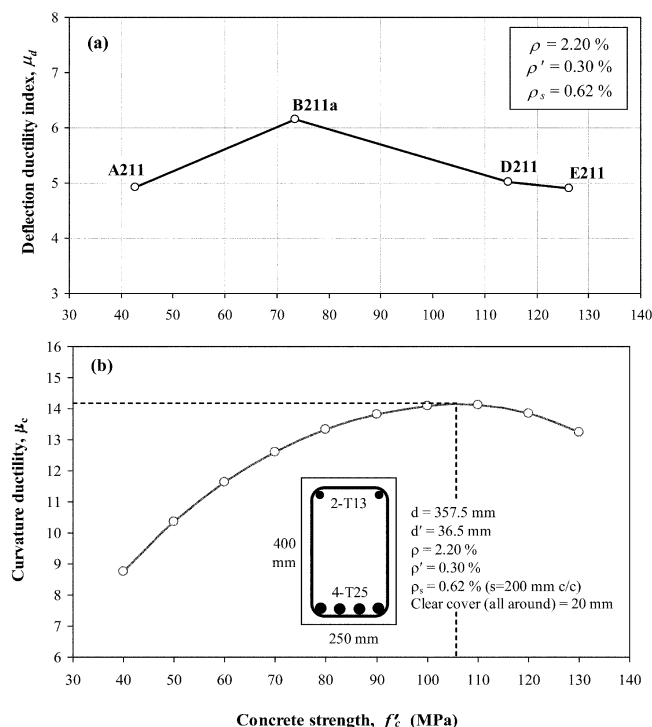


Fig. 3—Beam ductility as influenced by concrete strength: (a) test data; and (b) analytical values.

$$\rho_s = \frac{2(b'' + d'')A_s''}{b''d''s} \quad (8)$$

where A_s'' is the area of lateral ties; b'' and d'' are the width and depth, respectively, of confined concrete core based on the centerline of tie bars, and s is the spacing of tie bars.

Using equilibrium and Bernoulli's compatibility, analyses have been carried out by varying the concrete strength f'_c from 40 to 130 MPa at increments of 10 MPa. In the analysis, a representative stress-strain model for confined and unconfined HSC, as suggested by Mansur, Chin, and Wee³⁰ and Wee, Chin, and Mansur,³¹ respectively, and a bilinear stress-strain relation for steel have been employed. The curvature ductility indexes thus obtained are plotted against the concrete strength in Fig. 3(b). It may be clearly seen that ductility increases first with an increase in concrete strength, reaching a maximum value at $f'_c = 105$ MPa. Thereafter, any increase in concrete strength leads to a decrease in ductility. Concrete strength corresponding to this optimum ductility, however, is not the same as that observed experimentally (Fig. 3(a)), perhaps due to the differences in the definition of ductility. Nevertheless, the analysis supports the experimental trend.

Influence of tensile reinforcement on ductility—The most commonly used means of guaranteeing adequate ductility is by limiting the tensile reinforcement ratio ρ . According to the ACI Code,¹⁶ in a flexural member, ρ should be limited to $0.75\rho_{bs}$ for common situations and to $0.5\rho_{bs}$ for structures in which redistribution of moments is to be considered, where ρ_{bs} is the balanced steel ratio for a singly reinforced section. In the case of a doubly reinforced section, the aforementioned limitations should apply to $(\rho - \rho')$.

Assuming $E_s = 200$ GPa and $f_y = 460$ MPa, the requirement of $\rho \leq 0.5\rho_{bs}$ translates into a minimum curvature ductility

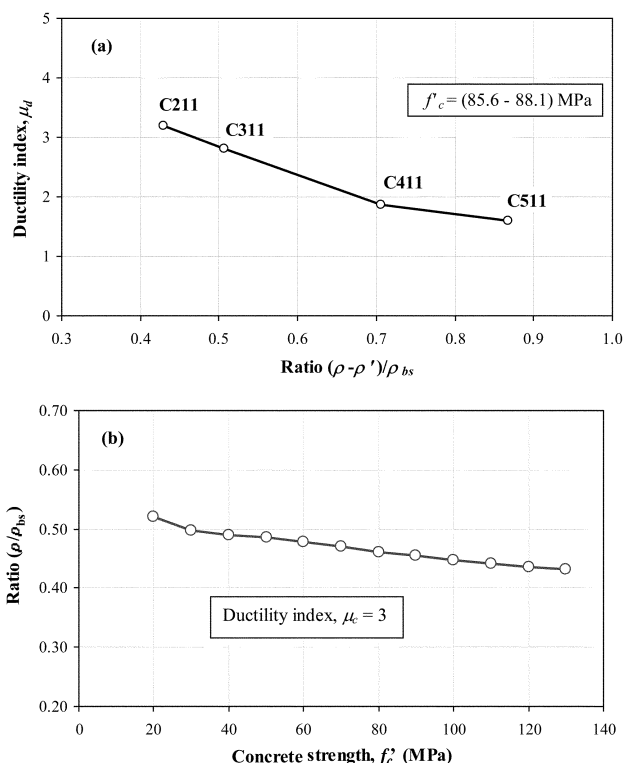


Fig. 4—Tensile reinforcement ratio and beam ductility: (a) test data; and (b) variation of reinforcement ratio requirement with variation in concrete strength for curvature ductility index of 3.0.

index μ_c of 3.0 for 30 MPa concrete in singly reinforced beams. The same number, 3.0, is also frequently referred to as the minimum requirement for the deflection ductility index μ_d in the study of RC beams.

To evaluate the performance of test beams with regard to the minimum ductility requirement, specimens in Series C are considered where the amount of tensile reinforcement was the only variable if the minor and unintentional variation in concrete strength is ignored. For these beams, deflection ductility index μ_d is expressed as a function of the reinforcement ratio $(\rho - \rho')/\rho_{bs}$, and is shown in Fig. 4(a). This figure clearly shows that the ductility index decreases as the amount of tensile reinforcement is increased, and the minimum target of $\mu_d = 3.0$ can be achieved at a value of approximately 0.45 for $(\rho - \rho')/\rho_{bs}$.

If 3.0 is considered as the target ductility index, then for a singly reinforced section, assuming $E_s = 200$ GPa and $f_y = 460$ MPa and following the ACI Code¹⁶ specifications, it can be analytically shown that the required value of ρ/ρ_{bs} decreases with the increase in concrete strength, as can be seen in Fig. 4(b). For higher concrete strength, ρ/ρ_{bs} goes well below the limit of 0.50. For example, a beam with $f'_c = 100$ MPa requires a reinforcement ratio of $\rho/\rho_{bs} = 0.45$ to attain the curvature ductility index of 3.0.

Higher-strength concrete is more brittle, and its ultimate compressive strain capacity (that is, concrete strain at the initiation of its crushing under compression) is less than that of lower-strength concrete. Also, the confinement is less effective for HSC than NSC because HSC undergoes less volume dilation in the inelastic range.³² Considering these characteristics of HSC, and in view of the preceding discussion, it is suggested that the maximum limit on tensile reinforcement be reduced to approximately $0.4\rho_{bs}$ when HSC with a

compressive strength of 100 MPa is involved. For the range of concrete strengths between 40 and 100 MPa, a linear interpolation between $0.5\rho_{bs}$ and $0.4\rho_{bs}$ may be considered.

Influence of compression reinforcement and lateral ties on ductility—In a flexural member, steel bars placed in the compression zone help reduce the depth of the neutral axis by virtue of their higher strength and modulus of elasticity than concrete, thus enhancing the beam's ability to deform before final collapse. They also participate, together with transverse ties, in confining the concrete in the compression zone. Such confinement increases the strain capacity of the concrete before it disintegrates, thus enhancing the ductility of a beam. The roles of compression reinforcement and lateral ties in boosting the capacity of a beam to deform without a significant strength loss are already well known and well established. Therefore, the following discussion concentrates on a qualitative evaluation of their influences based on test results generated in this study.

The combined effect of compression steel and lateral ties on member ductility observed in the present study is presented in Fig. 5(a), where μ_d has been plotted against the quantity $(\rho''f_y'')/f_c'$. Herein, ρ'' is the volumetric ratio of compressive and lateral tie steel expressed as follows

$$\rho'' = \rho_s + \frac{A'_s}{b''d''} \quad (9)$$

where ρ_s is the volumetric ratio of lateral tie steel as defined by Eq. (8); A'_s is the area of compressive steel. From Fig. 5(a), it may be seen that Beams B312, B321, and B331 show almost the same ductility. This is because improvement in member ductility depends on the effectiveness of both compressive steel and lateral ties.

The relative efficiency of lateral ties and compressive steel in increasing μ_d may be examined in Fig. 5(b) and (c). While Fig. 5(b) shows the ductility index as a function of $(\rho_s f_y'')/f_c'$, the variation of μ_d with $(\rho' f_y'')/f_c'$ is plotted in Fig. 5(c). Within the range of parameters considered in this study, it may be seen that an increase in ρ_s by decreasing the tie spacing, but with nominal compression reinforcement, can improve ductility of the beam (Fig. 5(b)). Contrary to expectation, however, an increase in the amount of compression reinforcement does not always lead to an improved ductility when nominal spacing of lateral ties is provided (Fig. 5(c)). This might be due to premature buckling (that is, buckling before yielding) of compression bars and consequent disintegration of the confined concrete core because of longer unsupported length ($s = 200$ mm).

The photographs of crushed cover concrete and the buckled compression bars in Beam C211 are shown in Fig. 6(a) and (b), respectively. This beam contained nominal ties at a spacing of $s = 200$ mm. At the initial stages of loading, strains in the compression bars increased smoothly with an increase in deflection (Fig. 6(c)). At one stage prior to yielding, however, the strain changed abruptly and followed an unusual variation indicating probable buckling of compression bars. This premature buckling is due to a larger unsupported length of compression bars. In contrast, the compression bars in Beams B312 ($s = 100$ mm) and B313 ($s = 67$ mm) yielded before buckling and displayed a linear variation of strains as can be seen in Fig. 6(d) and (e), respectively.

It may be mentioned herein that the nominal quantities of both compressive reinforcement and lateral ties (in terms of

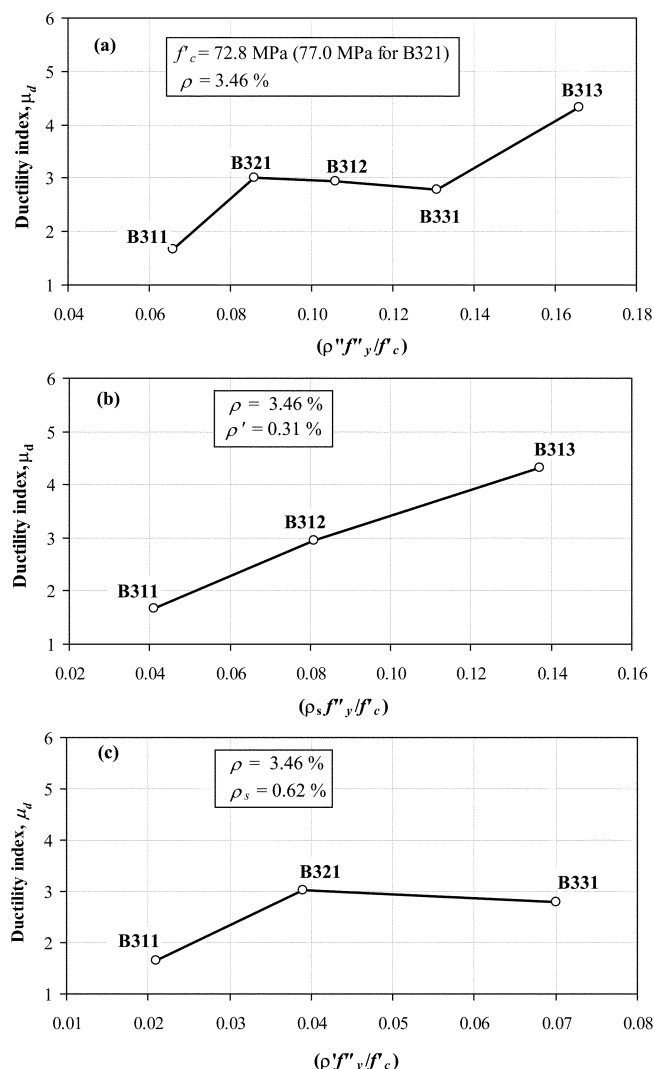


Fig. 5—Influence of compression reinforcement and tie steel on beam ductility: (a) combined effect; (b) tie spacing; and (c) compression reinforcement ratio.

maximum tie spacing) were considered in accordance with the provisions of the ACI Code.¹⁶ In the Code, the maximum tie spacing specified for a flexural member is the same as that required for a compression member. A compression member, however, is subjected to more or less uniform deformation, whereas the compression zone in a flexural member is subjected to a steep strain gradient. Due to this basic difference, the required buckling load for the compression bar in a flexural member may differ from that of a bar in a compression member. The eventual buckling failure of all the specimens with $s = 200$ mm tested in this program clearly demonstrates that this spacing is too large to allow the beam to attain its full deformation potential. Therefore, for critical sections in a flexural member, be it singly reinforced with nominal hanger bars on the compression side or doubly reinforced, the maximum spacing limit for lateral ties should be reduced from that specified in the ACI Code¹⁶ provisions.

In this respect, Park and Paulay¹⁸ suggested that the maximum spacing of closed ties in the plastic hinge zone of a RC member should be $d/4$ for proper moment redistribution. As discussed in the preceding paragraphs, the compression bars in Beam B313 in which tie spacing was less than $d/4$ did not show any premature buckling. The same is the case for Beam

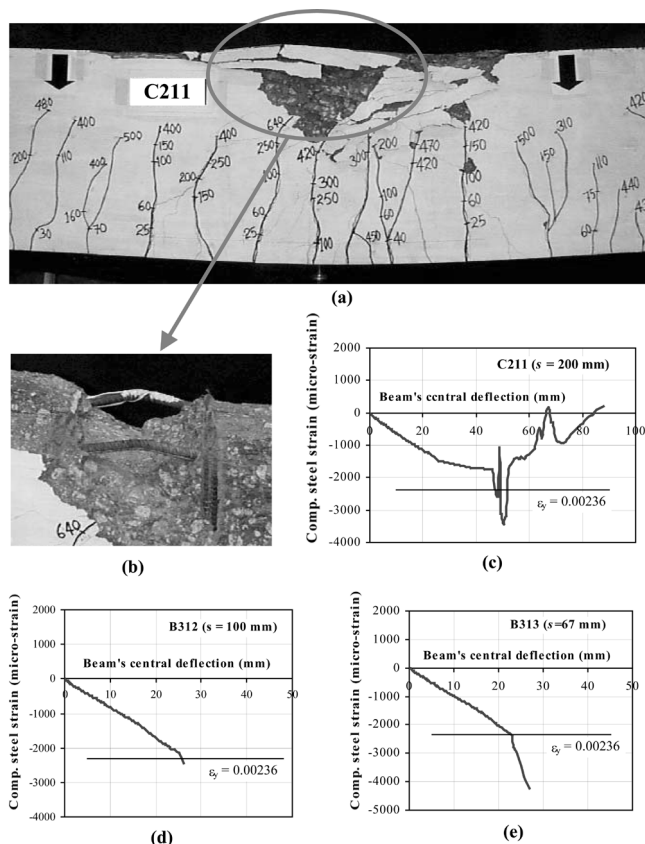


Fig. 6—(a) and (b) are photographs of failure zone and buckled compression reinforcement, respectively in Beam C211; and (c) to (e) are variations of strain in compression reinforcement in Beams C211, B312, and B313, respectively.

B312, where tie spacing was slightly larger than $d/4$. Therefore, conforming to the minimum size of compression bars, a maximum tie spacing equal to $d/4$ seems to be adequate to prevent premature buckling when ductility is the main point of concern.

CONCLUSIONS

The study reported in this paper mainly investigates the implications of using HSC in RC flexural members. Test data generated in this study, together with those collected from the literature, provided the necessary database for investigating all of the major issues concerning the flexural performance. Within the scope of this investigation, the following conclusions can be made:

1. The cracking moment capacity of a HSC beam is well predicted by the ACI Code¹⁶ without due considerations for shrinkage-induced stresses and the associated creep, the effects of which seem to be indirectly accounted for by using a conservative expression for modulus of rupture f_r ;
2. The ACI Code¹⁶ specifications are found to underestimate the maximum deflection of reinforced HSC beams at service load. A reasonable estimate can, however, be made by considering an age-adjusted modulus of elasticity and premature cracking of the beams due to shrinkage and associated creep of concrete;
3. At service load, maximum crack width is not significantly affected by the tensile reinforcement ratio ρ for the range employed in this study, but it increases as concrete strength is increased. Reasonable predictions for the maximum crack

widths in reinforced HSC beams can be obtained by using the well-known Gergely and Lutz²⁷ equation;

4. The equivalent rectangular stress block specified in the ACI Code¹⁶ and the failure criterion of $\epsilon_{cu} = 0.003$ have been found to give reasonable conservative predictions for the ultimate moment capacity of HSC beams with concrete strengths as high as 126 MPa;

5. For a fixed amount of reinforcement, the ductility of a beam has been found to increase with an increase in concrete strength f'_c , but up to a value of $f'_c = 105$ MPa. Beyond this, any increase in concrete strength leads to a reduction in ductility;

6. To attain a ductility index of 3.0, the lower limit of ductility as frequently referred to in the literature, the upper limit of $0.5\rho_{bs}$ on ρ or $(\rho - \rho')$ should be reduced as the concrete strength gets higher; for example, to $0.4\rho_{bs}$ when f'_c is 100 MPa; and

7. To ensure realization of full potential with respect to ductility, the ACI Code¹⁶ specifications for maximum spacing of ties in RC flexural members need to be reduced to $d/4$, particularly at critical sections. This will prevent premature disintegration of the confined concrete core in the compression zone due to buckling of compression reinforcement.

ACKNOWLEDGMENTS

The research reported in this paper is partly supported by Research Grant R-264-000-015-112, with funds given by National University of Singapore. The concrete used in this study was contributed by Pioneer Concrete (Singapore) Pvt. Ltd. The authors gratefully acknowledge this support.

REFERENCES

1. Ashour, S. A., "Effect of Compressive Strength and Tensile Reinforcement Ratio on Flexural Behavior of High-Strength Concrete Beams," *Engineering Structures*, V. 22, No. 5, 2000, pp. 413-423.
2. Mansur, M. A.; Chin, M. S.; and Wee, T. H., "Flexural Behavior of High-Strength Concrete Beams," *ACI Structural Journal*, V. 94, No. 6, Nov.-Dec. 1997, pp. 663-674.
3. Sarker, S.; Adwan, O.; and Munday, J. G. L., "High Strength Concrete: An Investigation of the Flexural Behavior of High Strength RC Beams," *The Structural Engineer*, V. 75, No. 7, 1997, pp. 115-121.
4. Pendyala, R.; Mendis, P.; and Patnaikuni, I., "Full-Range Behavior of High-Strength Concrete Flexural Members: Comparison of Ductility Parameters of High and Normal-Strength Concrete Members," *ACI Structural Journal*, V. 93, No. 1, Jan.-Feb. 1996, pp. 30-35.
5. Lin, C.-H.; Ling, F.-S.; and Hwang, C.-L., "Flexural Behavior of High Strength Fly Ash Concrete Beams," *Journal of the Chinese Institute of Engineers*, Taiwan, V. 15, No. 1, 1992, pp. 85-92.
6. Lambotte, H., and Taerwe, L. R., "Deflection and Cracking of High Strength Concrete Beams and Slabs," *High-Strength Concrete*, Second International Symposium, SP-121, W. T. Hester, ed., American Concrete Institute, Farmington Hills, Mich., 1990, pp. 109-128.
7. Paulson, K. A.; Nilson, A. H.; and Hover, K. C., "Immediate and Long-Term Deflection of High Strength Concrete Beams," *Research Report No. 89-3*, Department of Structural Engineering, Cornell University, Ithaca, N.Y., 1989, 230 pp.
8. Marro, P., "Bending and Shear Tests Up to Failure of Beams Made with High-Strength Concrete," *International Symposium on Utilization of High Strength Concrete*, Stavanger, Norway, June 15-18, 1987, pp. 183-193.
9. Uzumeri, S. M., and Basset, R., "Behaviors of High Strength Concrete Members," *International Symposium on Utilization of High Strength Concrete*, Stavanger, June 15-18, 1987, Norway, pp. 237-248.
10. Shin, S.-W., "Flexural Behavior Including Ductility of Ultra-High-Strength Concrete Members," PhD thesis, University of Illinois at Chicago, Ill., 1986, 232 pp.
11. Swamy, R. N., "High-Strength Concrete—Material Properties and Structural Behavior," *High-Strength Concrete*, SP-87, H. G. Russell, ed., American Concrete Institute, Farmington Hills, Mich., 1985, pp. 119-146.
12. Pastor, J. A.; Nilson, A. H.; and Slate, F. O., "Behavior of High Strength Concrete Beams," *Research Report No. 84-3*, Department of Structural Engineering, Cornell University, Ithaca, N.Y., 1984, 311 pp.
13. Okada, K., and Azimi, M. A., "Strength and Ductility of Reinforced High Strength Concrete Beams," *Memoirs of the Faculty of Engineering*,

Kyoto University, Japan, V. 43, No. 2, 1981, pp. 304-318.

14. Tognon, G.; Ursella, P.; and Coppetti, G., "Design and Properties of Concretes with Strength over 1500 kgf/cm²," *ACI JOURNAL, Proceedings* V. 77, No. 3, May-June 1980, pp. 171-178.

15. Leslie, K. E.; Rajagopalan, K. S.; and Everard, N. J., "Flexural Behavior of High Strength Concrete Beams," *ACI JOURNAL, Proceedings* V. 73, No. 9, Sept. 1976, pp. 517-521.

16. ACI Committee 318, "Building Code Requirements for Structural Concrete (ACI 318-02) and Commentary (318R-02)," American Concrete Institute, Farmington Hills, Mich., 2002, 443 pp.

17. ACI Committee 363, "State-of-the-Art Report on High Strength Concrete (ACI 363R-92)," American Concrete Institute, Farmington Hills, Mich., 1992, 55 pp.

18. Park, R., and Pauley, T., *Reinforced Concrete Structures*, John Wiley and Sons, New York, 1975, pp. 195-269.

19. Shin, S.-W.; Ghosh, S. K.; and Moreno, J., "Flexural Ductility of Ultra-High-Strength Concrete Members," *ACI Structural Journal*, V. 86, No. 4, July-Aug. 1989, pp. 394-400.

20. Rashid, M. A.; Mansur, M. A.; and Paramasivam, P., "Correlations Between Mechanical Properties of High Strength Concrete," *Journal of Materials in Civil Engineering*, ASCE, V. 14, No. 3, May-June 2002, pp. 230-238.

21. Ghali, A., "Deflection of Reinforced Concrete Members: A Critical Review," *ACI Structural Journal*, V. 90, No. 4, July-Aug. 1993, pp. 364-373.

22. Gilbert, R. I., "Deflection Calculation for Reinforced Concrete Structures—Why We Sometimes Get It Wrong," *ACI Structural Journal*, V. 96, No. 6, Nov.-Dec. 1999, pp. 1027-1032.

23. Gilbert, R. I., "Serviceability Considerations and Requirements for High Performance Reinforced Concrete Slabs," *International Conference*

on High Performance High Strength Concrete, Perth, Australia, Aug. 1998, pp. 425-439.

24. Large, G. E., and Chen, T. Y., *Reinforced Concrete Design*, The Ronald Press Co., New York, 1969, pp. 481-497.

25. Gilbert, R. I., *Time Effects in Concrete Structures*, Elsevier Science Publishers B. V., Amsterdam, The Netherlands, 1988, pp. 59-89.

26. Branson, D. E., "Instantaneous and Time-Dependent Deflections of Simple and Continuous Reinforced Concrete Beams," *Report No. 7, Part I*, Alabama Highway Research Department, Bureau of Public Roads, 1963, pp. 1-78.

27. Gergely, P., and Lutz, L. A., "Maximum Crack Width in Reinforced Concrete Flexural Members," *Causes, Mechanism, and Control of Cracking in Concrete*, SP-20, R. E. Philleo, ed., American Concrete Institute, Farmington Hills, Mich., 1968, pp. 87-117.

28. BS 8110, "Structural Use of Concrete: Part 2: Section 3," British Standards Institution, London, 1985.

29. Scott, B. D.; Park, R.; and Priestley, M. J. N., "Stress-Strain Behavior of Concrete Confined by Overlapping Hoops at Low and High Strain Rates," *ACI JOURNAL, Proceedings* V. 79, No. 1, Jan.-Feb. 1982, pp. 13-27.

30. Mansur, M. A.; Chin, M. S.; and Wee, T. H., "Stress-Strain Relationship of Confined High-Strength Plain and Fiber Concrete," *Journal of Materials in Civil Engineering*, ASCE, V. 9, No. 4, 1997, pp. 171-179.

31. Wee, T. H.; Chin, M. S.; and Mansur, M. A., "Stress-Strain Relationship of High-Strength Concrete in Compression," *Journal of Materials in Civil Engineering*, ASCE, V. 8, No. 2, 1996, pp. 70-76.

32. Ahmad, S. H., and Shah, S. P., "Structural Properties of High Strength Concrete and Its Implications for Precast Prestressed Concrete," *PCI Journal*, V. 30, No. 4-6, 1985, pp. 92-119.

Reproduced with permission of the copyright owner. Further reproduction prohibited without permission.